Fractured 3D Object Restoration and Completion

A. Andreadis[1] R. Gregor[2] I. Sipiran[2] P. Mavridis[1] G. Papaioannou[1] T. Schreck[2]

[1]Athens University of Economics & Business [2]University of Konstanz

SIGGRAPH 2015

This work was supported by EC FP7 STREP Project PRESIOUS, grant no. 600533.

Motivation and Problem Statement

The problem of object restoration from eroded fragments, where large parts could be missing, is of high relevance in archaeology. Manual restoration is possible and common in practice but it is a tedious and error-prone process, which does not scale well. Solutions for specific parts of the problem have been proposed but a complete reassembly and repair pipeline is absent from the bibliography. We propose a shape restoration pipeline consisting of appropriate methods for automatic fragment reassembly and shape completion. We demonstrate the effectiveness of our approach using real-world fractured objects.

Method Overview

We extend, instantiate and apply our preliminary restoration pipeline described earlier in [2]. We suggest two main restoration phases (see also the diagram below). In the first phase, fragments are reassembled. The reassembly solution results from finding the Minimum Spanning Tree 3 for pairwise matches between fragment contact surfaces 2 which have been identified in a preprocessing step 1. The reassembly is guided by global error relaxation and can also make use of external feature curves on the fragments 1. The obtained reassembly solution typically misses some parts of the shape, due to missing or eroded fragments. Therefore, in the second phase we compute plausible complete versions of the reassembles partial shapes. This is done by robust detection of global shape symmetries which relies on local shape features 4.b. Completion of non-symmetric shapes is assisted by template repair shapes retrieved by a partial 3D similarity search 4.a. The final shape is finished by merging and smoothing of the obtained parts 5, inpainting of missing local shape information, and export of synthesized missing parts for physical restoration 7.

Results

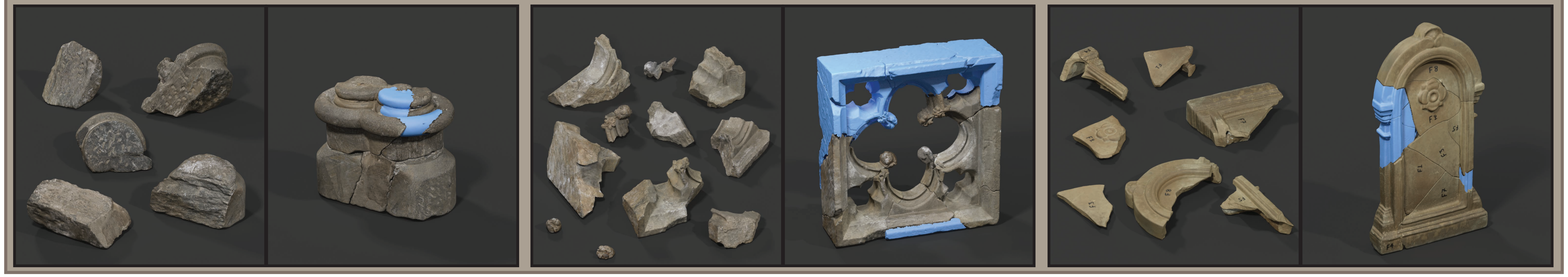

Reassembly & Repair Pipeline

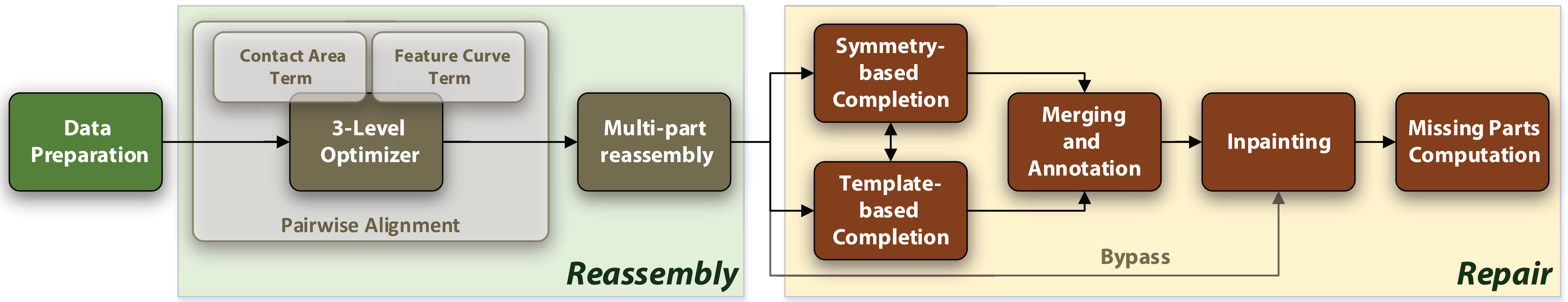

1 - Data Preparation

Facet Extraction & Classification: We use a standard region-growing procedure, which produces regions separated by sharp edges, using as the stopping criterion the deviation of averaged normals. Regions with a high variance in the *bending energy* are then classified as potential fracture facets and are tagged for matching against fractured surfaces of other fragments.

Distance Field Pre-Computation: In order to speed up the distance queries required by the next steps of the pipeline, fragments are discretely sampled on a 3D grid extending over the narrow band of their surface, and stored using a sparce hierarchical volumetric data structure, the VDB.

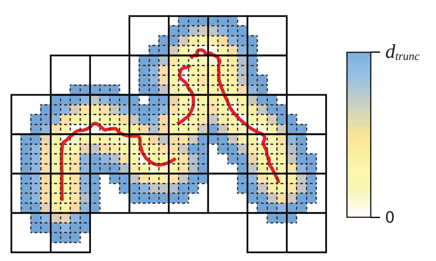

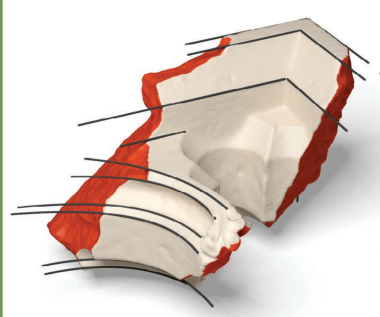

Feature-Curve Extraction: Feature curves spanning across multiple fragments are extracted from the intact surfaces, to address the pairwise-matching problems which are hard or impossible to solve using contact surface.

Initially feature points are extracted and organized into connected groups. The feature curve of each group is extracted using a skeletonization approach and subsequently approximated with B-Splines, which are used to extrapolated features beyond the fractured facets.

2 - Pairwise Alignment

Objective Function: Given two discretized surfaces, the source $\mathcal{X}$ and target $\mathcal{Y}$, the extrapolated feature points $\mathcal{E}$ associated with $\mathcal{X}$ and the surface feature points $\mathcal{S}$ associated with $\mathcal{Y}$, we formulate the problem as a minimization problem:

$$\arg\min_{\mathbf{R},\mathbf{t}} \left(c\sum_{j=1}^{k} w_j\phi(\mathbf{R}\mathbf{e}_j+\mathbf{t},\mathcal{S}) + (1-c)\sum_{i=1}^{n}\phi(\mathbf{R}\mathbf{x}_i+\mathbf{t},\mathcal{Y})\right) + I_{SO(3)}(\mathbf{R})$$

k,n : the number of points of $\mathcal{E}$ and $\mathcal{X}$ respectively
c : the relative contribution of the features term
w_j : exponential falloff weighting term
$\mathbf{R},\mathbf{t}$: rotation matrix $\in\mathbb{R}^{3\times3}$ and translation vector $\in\mathbb{R}^3$
$I_{SO(3)}(\mathbf{R})$: enforces the rigidity of the transformation

L_p-norm Formulation: The function $\phi(\mathbf{a},\mathcal{B})$ measures the distance of an arbitrary point $\mathbf{a}\in\mathbb{R}^3$ to the surface $\mathcal{B}$ and is defined as:

$$\phi(\mathbf{a},\mathcal{B}) = \min_{\mathbf{b}\in\mathcal{B}} \phi(\mathbf{a},\mathbf{b})$$

where $\phi(\mathbf{a},\mathbf{b})$ measures the distance between two points, using the ℓ_p-norm. For small values of p the optimizer becomes robust to outliers.

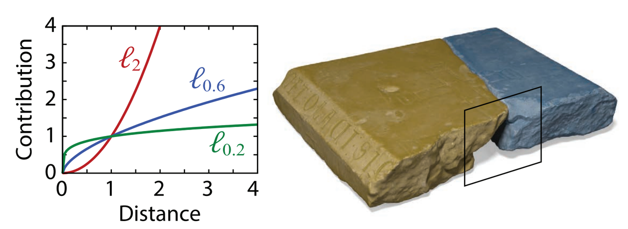

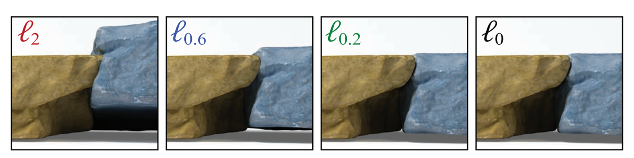

Optimization Strategy: We utilize a 3 level coarse-to-fine optimization [1]:

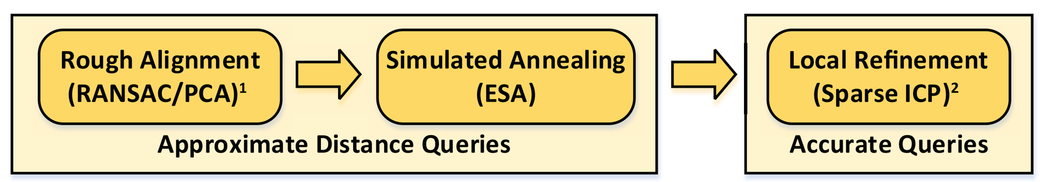

[1] When the surface area of two facets is roughly equal we align them using PCA. Otherwise a RANSAC-based alignment procedure is used.

[2] Depending on the coverage of the facets area the Sparse ICP is performed either on the surface data or the external feature sets.

Pairwise Alignments:

3 - Multi-part Reassembly

Multi-part Reassembly: A weighted graph with one vertex per fragment, and pairwise matches as edges is built. The *Minimum Spanning Tree* is extracted through Kruskal's algorithm and using penetration tests and edge discards we ensure penetration-free only reassemblies. Manual constrains are also supported.

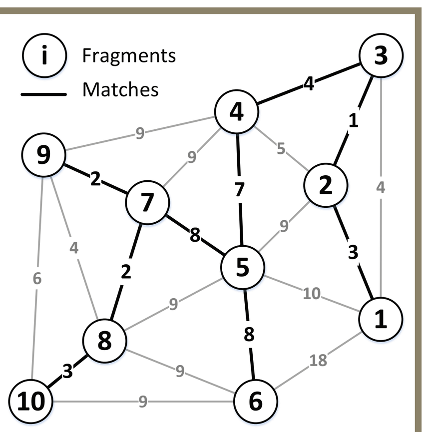

Global Error Relaxation: An iterative relaxation process is used to adjust the final transformation of fragments.

Multi-part Reassemblies:

4.a - Template-based Completion

The template-based Completion relies on external similarity of the reassembled fragment set to template shapes in a repository. In our approach, the template repository is populated by arbitrary sources such as randomized instances of parametric surfaces, digitized CH objects or CAD models.

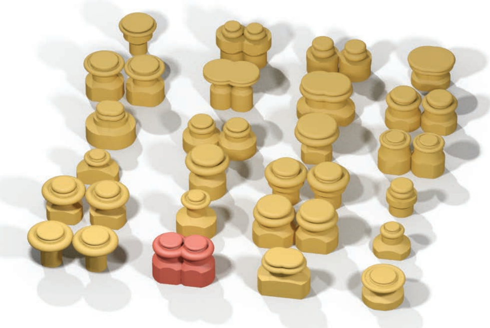

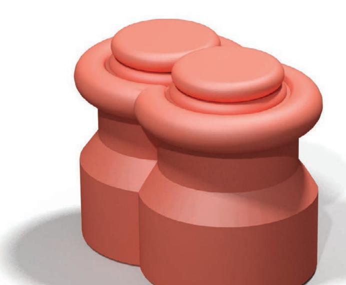

Template Retrieval: Custom variations of *Heat Kernel Signatures* are encoded using a *Spatially Sensitive Bag of Features* approach (SS-BoF), roughly similar to [4]. This approach, has been shown to deliver state-of-the-art retrieval performance when robustness against e.g. local perturbations, sampling differences and noise is crucial. In addition to the SS-BoF descriptors, for Query and Template, F_Q and F_T, we compute a second weighted SS-BoF variation F_{Qw} which exploits the surface classification that has been established in the data preparation step. Features that stem from patches with a low biharmonic distance to areas classified as breaking edges obtain a lower weighting in the encoding process. The distance between the reassembled fragment set and each template is obtained by the following metric, where α can be used to control the impact of F_Q and F_{Qw} on the final distance.

$$d_f(Q,T) = L_1(F_{Qw},F_T) + \alpha\frac{L_1(F_{Qw},F_T) - L_1(F_Q,F_T)}{L_1(F_{Qw},F_T) + L_1(F_Q,F_T)}$$

Template Alignment: Retrieved objects are now aligned to the input fragments. We obtained promising results by applying Sparse ICP after optimizing similarity, inspired by [6], where we optimize the D2 shape distribution of the template, parametrized for affine transformations. A *non-rigid* registration method for finding alignments beyong affine transformations is currently work in progress.

4.b - Symmetry-based Completion

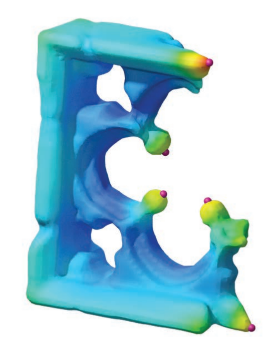

Symmetric Correspondences: We compute a difussion-based function (*Heat Kernel)* over a shape $\mathcal{X}$ that preserves local symmetries [3].

$$\mathcal{H}_t(x) = \sum_{i=0}^{\infty}\left(\frac{1-e^{-\lambda_i t}}{\lambda_i}\right)\vec{v}_i(x)^2$$

where x the analyzed vertex, t the difussion time, and λ_i and $\vec{v}_i$ the eigenvalues and eigenvectors of the *Laplace-Beltrami* operator of $\mathcal{X}$.

Our method selects the local maxima of $\mathcal{H}_t(x)$ (evaluated in low values of t) as candidate symmetric points.

Detection of Planes: Every pair of selected points generates a candidate plane. In order to determine if this plane is good, our method accumulates votes by using high-curvature points on the surface. Criteria for good votes are the distance to plane, normal coherence, distance in feature space, just to name a few. Candidate planes with high votes are selected.

Symmetric Transformation: Our method computes the reflection with respect to the best plane. As the symmetry plane is only approximated, a final registration step is required to fit the original model with the reflected one as much as possible.

5 - Merging and Annotation

After missing geometry has been inferred by template- and symmetry-based completion, all fragments from the reassembly and the inferred geometry are merged into a single manifold using boolean operations. During this step, the origin of each vertex, along with its distance to nearest neighbors of different origins, is preserved by annotations.

6 - Inpainting

This step provides the final repaired object and while it is currently work in progress, it is based on the automation of an existing, user-driven technique for detail transfer across geometric shapes [5], which is well suited even for transfer of very complex local geometry. Similar areas stemming from intact surface parts and inferred geometry are automatically selected in order to transfer local detail on the breaking edges and gaps of the merged shape. Distinction between source and target areas is based on annotations from the merging step, where similar patches are identified using diffusion based features.

7 - Missing Parts Computation

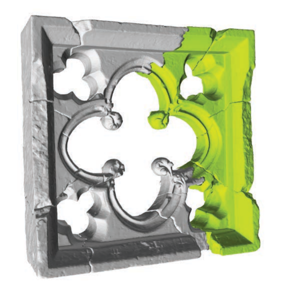

Once the object has been repaired, missing parts are computed by a boolean operation that subtracts the reassembled fragments from the repaired object. The remaining parts could e.g. be used for reproduction by 3D printers after device specific post-processing.

References

[1] Mavridis, P., Andreadis, A., Papaioannou, G. 2015. Fractured object reassembly via robust surface registration. In (To appear) Eurographics Conference (short paper), EG.
[2] Gregor, R., Sipiran, I., Papaioannou, G., Schrect, T., Andreadis, A., and Mavridis, P. 2014. Towards automated 3D reconstruction of defective cultural heritage objects. In Ws. on Graphics and Cultural Heritage, EG, 135–144.
[3] Sipiran, I., Gregor, R., and Schreck, T. 2014. Approximate symmetry detection in partial 3D meshes. Computer Graphics Forum 33, 7, 131–140.
[4] Bronstein, A. M., Bronstein, M. M., Guibas, L. J., and Ovsjanikov, M. 2011. Shape google: Geometric words and expressions for invariant shape retrieval. ACM Transactions on Graphics 30, 1 (Feb.), 1:1-1:20.
[5] Takayama, K., Schmidt, R., Singh, K., Igarashi, T., Boubekeur, T., and Sorkine, O. 2011. Geobrush: Interactive mesh geometry cloning. Computer Graphics Forum, 30, 613-6232.
[6] Ovsjanikov, M., Li, W., Guibas, L., & Mitra, N. J. (2011). Exploration of continuous variability in collections of 3D shapes. ACM Transactions on Graphics (TOG), 30(4), 33.